Int. J. Heat Mass Transfer. Vol. 26, No. 10, pp. 1479-1488, 1983
Printed in Great Britain

0017-9310/83 $3.00 + 0.00

EVAPORATIVE CONVECTION IN MINUTE DROPS ON A PLATE WITH TEMPERATURE GRADIENT

NENGLI ZHANG* and WEN-JEI YANG
Department of Mechanical Engineering & Applied Mechanics, The University of Michigan, Ann Arbor, MI 48109, U.S.A.

(*Received* 12 *October* 1982 *and in final form* 21 *January* 1983)

Abstract—Thermal convection in a minute drop evaporating on a plate surface is visualized through two methods: solid suspension and laser shadowgraphy. The plate is partially heated to create a temperature field on the test site so that the Marangoni effect may be induced on the drop surface. Through altering plate inclination, the evaporating drop may stay at rest at the same spot or move on the plate. The observation of flow patterns in a stationary drop reveals that the presence of both surface tension and buoyancy forces lead to four distinct flow regimes in the drop with the buoyancy-driven convection on the warm side and the surface tension driven instability on the cold side. The effects of drop motion, liquid properties and air–liquid interfacial geometry on both the interfacial and internal flow structures are determined and the consequences of the evaporation rate are discussed.

1. INTRODUCTION

THE INTERFACIAL turbulence, the motion of the interface between two phases, occurs when a gradient of chemical potential, such as temperature and/or concentration gradients, exists in the neighborhood of the interface. In other words, heat and/or mass transfer across an interface tends to induce interfacial turbulence. This is typically observed in a liquid surface undergoing evaporation. The surface flow phenomenon does not produce reflective index variation that can be seen by the naked eye.

Numerous studies have been reported on the thermal stability of flat interfaces between two phases of either infinite extent or finite layers. Both theoretical and experimental approaches have been undertaken (e.g. refs. [1, 2]). Sternling and Scriven [1] analyzed a hydrodynamic instability model to explain the mechanism of interfacial turbulence between two unequilibrated liquids. By means of the Schlieren technique, Berg *et al.* [2] identified a variety of convection patterns in layers of evaporating liquids; some being induced by a surface-tension driven instability while others being induced by a buoyancy driven convection. The observed flow structures were largely dependent upon the depth of the evaporating pool and to a much lesser extent on the properties of the liquid. When the interface is curved, as seen in a spherical drop in suspension or in a droplet on a solid surface, mathematical treatment and experimental observation of the interfacial flow phenomenon become more difficult. Han and Yang [3, 4] predicted the criteria for surface tension induced marginal instability in a hemispherical drop on a heated surface and for spherical liquid shells, respectively. Using the methods of direct photography and laser shadowgraphy, Zhang and Yang [5] revealed three flow structures at the liquid–air interface of a minute drop evaporating on a flat plate: stable, substable and unstable. Thus, an interfacial flow map was constructed and the mechanism of evaporation enhancement was determined.

The present study is concerned with thermal convective patterns in minute drops evaporating on a plate with an almost linear temperature field. The temperature field is to create a surface tension/temperature gradient on the drop surface so that through the Marangoni effect, the drop may move on the plate in horizontal position. The plate may be inclined to arrest the evaporating drop. The purpose of the study is to determine the effects of drop motion, air–liquid interfacial geometry and liquid properties on flow structures in the evaporating liquid. Both the solid suspension method and laser shadowgraphy are employed for flow observations.

2. EXPERIMENTAL METHODS AND RESULTS

Two methods were employed to visualize the convective patterns in a drop evaporating on a partially heated plate. The first was a suspension method using fine aluminum pigments as a tracer. The second method utilized the laser shadowgraphy of a drop lens.

2.1. *Aluminum suspension method*

The apparatus consisted of a white light source, a glass plate coated with developed emulsion on one side and a movie camera, as shown in Fig. 1. The developed emulsion had a specific density such that the photographic density was approximately 1.7. A strip of thermofoil heater was firmly attached to the underside of the test plate.

Throughout the entire study, the electric power input was set at a desired level with the corresponding lateral (perpendicular to the heater strip) temperature distribution measured in the absence of an evaporating drop. Five gauge number 32 copper–constantan thermocouples lined up along the center line were used to measure the plate surface temperature. They were placed on the upper-side of the test plate under an

* Visiting scholar on leave from the Department of Thermal Engineering, Tsinghua University, Beijing, China.

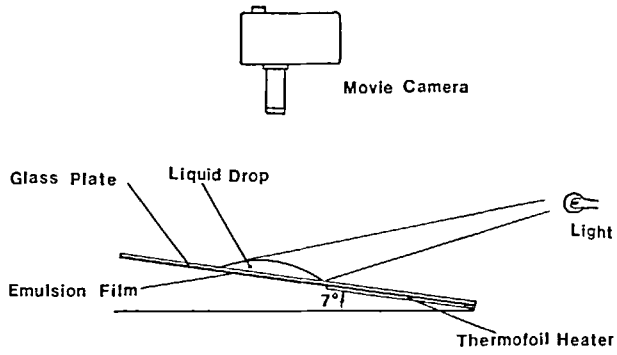

FIG. 1. A schematic diagram of direct photography.

insulating tape and firmly pressed onto the plate surface. Figure 2 depicts the steady temperature distribution monitored by the thermocouples whose location was marked by circles. Here the distance L was measured from the edge of the heating strip which was attached on the underside of the test plate. In order to keep the drop at rest during the observation and recording period, the test plate was tilted at a small angle, approximately 7°, from the horizontal position. A tiny amount of aluminum pigment 1400 was spread on the test plate. A minute drop of 8 μl size was carefully placed on the aluminum powder using a 50 μl Monojet microsyringe. The process may be reversed, that is, sprinkling the aluminum particles on a drop being placed on the glass surface. Both procedures eventually produced a fine suspension of solid particles in an evaporating drop. The flow pattern was recorded by a 16 mm Bolex H16 EBM movie camera using a Nikon Nikkor 300 mm 1:4.5 lens, on top of which a Kalt 72 mm Close-Up Diopter lens was mounted. The light source and the camera were situated at proper positions to produce a sharp contrast in the image of the flow patterns.

Figure 3 is a sequence of photos which illustrates the change in the shape of an ethyl acetate drop after it was placed on the plate at $L = 0$. The drop moved toward the colder (unheated) side of the plate due to the Marangoni effect; this effect was induced by local variations in the surface tension on the drop surface. During its migration process, the drop produced a tail which broke up and disappeared through evaporation. The drop came to a full stop, as shown in the last two photos when the balance of forces between the surface tension and gravity was achieved. The drop continued to evaporate thereafter until it completely disappeared. Different drops stopped at different locations depending on the liquid and its initial size. In order to visualize the flow patterns during evaporation, a small amount of fine aluminum powder was carefully placed on top of the drop surface. Immediately thereafter, one observed traces of the flow on the drop surface. Figure 4 depicts a schematic diagram of flow patterns in a stationary drop evaporating on an inclined plate (at a 7° angle). The flow patterns observed by the naked eye can be classified into four regions. On the warm side of the drop was a vast space of relatively strong flow-circulation which was buoyantly controlled. In region I, cold fluid fell along the drop surface while warm fluid, after being heated by the plate surface, rose through the interior of the drop volume, thus forming a circulating route along the same longitude. The drop surface in this region was relatively placid while active evaporation occurred because of exposure to the warm liquid stream. Region IV was small; it encompassed the area at the tip of the cold side where a pair of vortices was observed. The flow was governed by a surface tension force, referred to as the Marangoni stability. In this region the interface was appreciably agitated while the evaporative process was slow because of lower surface temperature and lack of internal flow circulation. Region III was located near the top of the drop where its two vortices ran counter-current with the vortex pair of region IV. These vortices served to promote heat exchange between the warm and cold streams through mixing. Region II, which had a feather-like flow pattern, was observed on the hillside of the drop situated between the warm and cold regions. The flow stream carried the heat from the warm to the cold side. The fluid motion in regions III and II was influenced by both buoyancy and surface tension mechanisms.

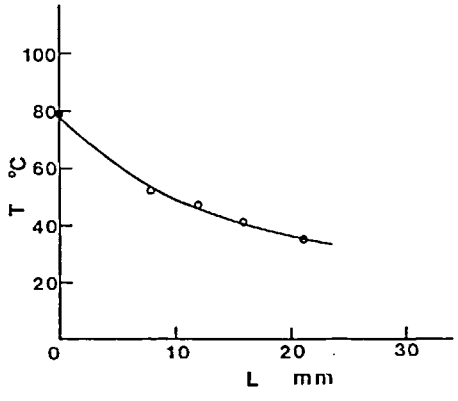

FIG. 2. Temperature distribution of plate surface with L measuring the distance from the edge of heating strip (circles indicate the location of thermocouples).

Figure 5 is a photograph of a chloroform drop taken

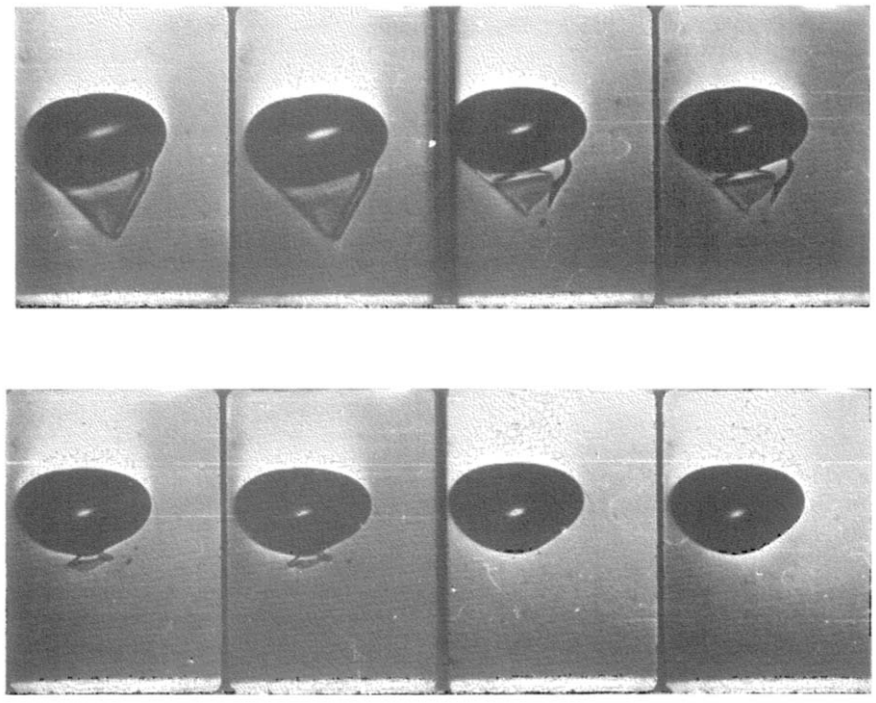

FIG. 3. Change of shape of an ethyl acetate drop during its motion from warm to cold side.

at a shutter speed of 1/100 s and $f = 16$. The flow pattern was made visible by suspending aluminum powders. Two vortices appeared in the third region. The faint vertical line image at the central position was the surface stream of the main flow circulation in region I. The oval area immediately below region I was merely a reflection of the illumination, while the bright image at the bottom position was the deposition of the aluminum powder left behind by liquid evaporation. In general, the image was less bright on the cold side than on the warm side because of weaker natural convection. The regions of weak flow would not appear in the photo.

2.2. *Laser shadowgraphic method*

The presence of contamination in the liquid would result in the suppression of the surface tension driven instability, although it could not affect the buoyancy driven convection. Therefore, the use of an aluminum-powder suspension in the drop is not desirable for visualization of the flow pattern which is brought about by a surface tension driving force.

2.2.1 *Experimental set-up.* The interfacial flow structures, which normally go unnoticed when viewed by the naked eye, can now be visualized through the use of laser shadowgraphy. This method has been described elsewhere [5]. The apparatus used in the laser shadowgraphy consisted of a laser light, a test plate with a strip of thermofoil heater attached to its underside, two aluminized mirrors, an indexed screen, and a camera, as shown in Fig. 6. The light, produced by a C.W. Radiation Model SP 2, 2.5 mW cylindrical helium–neon laser, passed through an achromatic

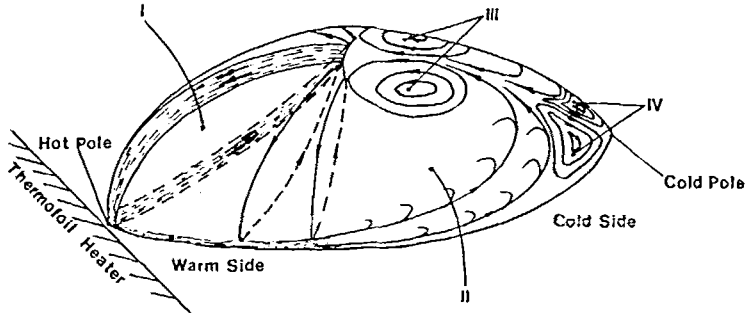

FIG. 4. A schematic diagram of flow patterns in a stationary drop evaporating on an inclined plate (at a 7° angle) with a temperature field.

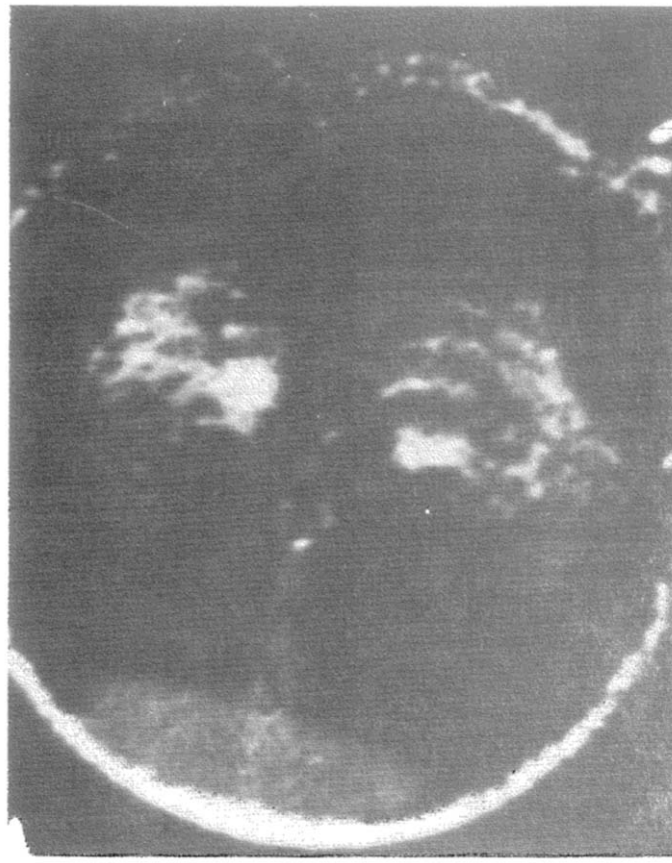

FIG. 5. A photograph of a chloroform drop with flow patterns visualized by suspending fine aluminum powders.

objective and a 10 micron-diameter pinhole and was then condensed by a collimating lens into a parallel beam. The two mirrors were aluminized on the surface facing the subject being studied so that the light could be reflected with no refraction. They were mounted in parallel at 45°. Heating was provided and the five plate temperatures were measured in the same manner as previously mentioned. The test plate without emulsive film coating was inserted between the two mirrors at a small angle from the horizontal position. The optical path from the lower mirror was horizontal and was intercepted by a vertical screen. The image on the screen

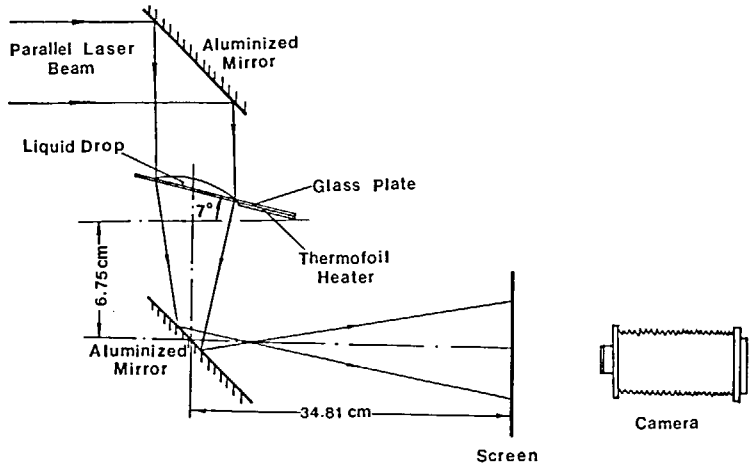

FIG. 6. A schematic diagram of the laser shadowgraphic system.

was recorded using either the movie camera or a Graphic View 162 mm Graflex Optar $f/4.5$ camera. Still photos were taken using high speed Polaroid Land film type 57 (ASA 3000).

2.2.2. *Qualitative interpretation of the shadowgraphic image.* Figures 7(a)–(c) are the shadowgraphs, taken at a shutter speed of 1/50 s and $f/4.5$, of a carbon tetrachloride drop at three different stages in the evaporation process. The plate temperature was at 51.3°C (the drop location can be found from Fig. 2) with a temperature gradient (dT/dL in Fig. 2) of 1.57°C mm^{-1}. The dark spot at the photo center was the shadow of the drop, while the surrounding dark circle represented the outer edge of the aperture (not shown in Fig. 6). The laser beam cast a bright background around the dark circle. The outermost periphery portrayed the flow structure at the air–liquid and liquid–solid interfaces of the drop. The area within the periphery was the shadow of the internal flow pattern with the drop produced by an optical effect of the temperature variation. The initial drop volume at contact was 9 μl with a diameter of approximately 4 mm on the plate surface. The images in Figs. 7(a)–(c) were magnified approximately 20 times. Owing to the density increase (compared to the surrounding air), the drop volume acted in a way similar to a convex lens. A darker region represented the shadow of the disturbance (higher second derivative of the refractive index than its neighborhood) through which a ray had passed and therefore corresponded to the recorder turbulent motion on the drop interface. The faint circular spots seen were the image of microdusts on the plate and were picked up using super-sensitive film, while the concentric rings near the outer periphery represented the image of the lens-shaped drop contours.

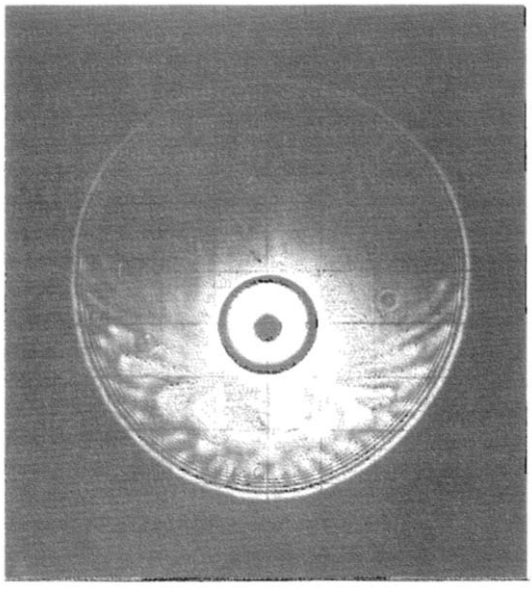

FIG. 7 (a).

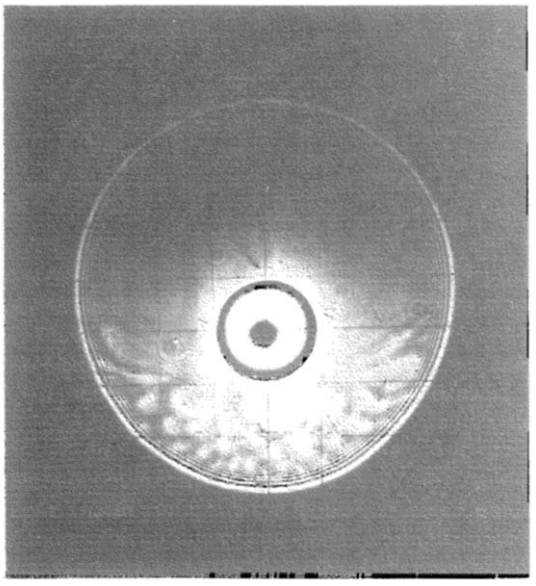

FIG. 7 (b).

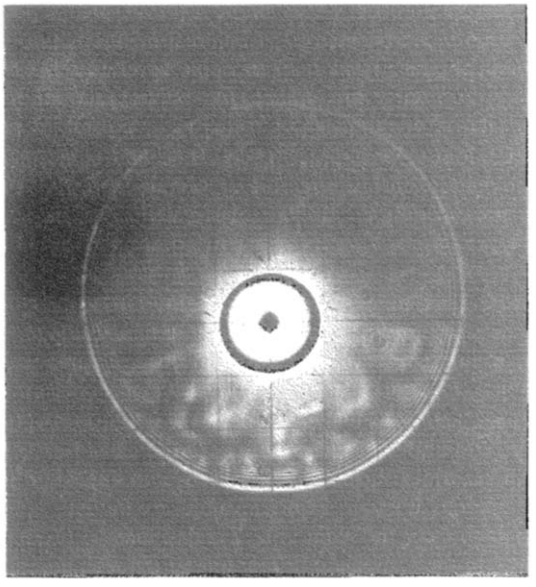

FIG. 7(c).

FIG. 7. Shadowgraphs of a carbon tetrachloride drop at (a) early stage, (b) intermediate stage, and (c) late stage of the evaporating process.

As it is well known, the shadowgraphic image is a pattern of light and dark regions constituting a map of the second derivative of the refractive index within the transparent subject under study. Since the refractive index of a fluid is a function of its temperature, the shadowgraphic image is an indirect indication of the distribution of temperature in the drop. It can thus be qualitatively stated that the warm side (seen in the upper part of the photo) of the drop is almost uniform in temperature as a result of strong buoyancy driven convection, as indicated by the nearly uniform dark

image in the shadowgraph. On the other hand, the cold end of the drop (seen in the lower part of the photo) has complex temperature variation which induces a surface tension driven instability, as evidenced by the feather-like pattern in the shadowgraphic image. This internal substructure continued to vary actively with time. In general, the cold side of the drop surface gradually became inactive, i.e. the nonuniformity of the temperature on the cold side was gradually weakened in the course of evaporation, as shown in Figs. 7(a)–(c).

2.2.3. *Effect of liquid properties.* Figure 8 depicts the shadowgraphic images of various liquid drops: (a) cyclohexane (at initial drop size = 9 μl; shutter speed = 1/100 s with $f/5.6$; plate temperature = 40.3°C with $dT/dL = 1.22°C\,mm^{-1}$), (b) ethyl ether (9 μl; 1/50 s and $f/4.5$; 42°C with $1.37°C\,mm^{-1}$), (c) methylene chloride (12 μl; 1/50 sec and $f/4.5$; 51.3°C with $2.03°C\,mm^{-1}$), (d) ethyl acetate (9 μl; 1/100 s and $f/5.6$; 46.6°C with $1.6°C\,mm^{-1}$), (e) chloroform (9 μl; 1/50 s and $f/4.5$; 51.3°C with $2.03°C\,mm^{-1}$), (f) benzene (9 μl; 1/100 s and $f/5.6$; 46.6°C with $1.6°C\,mm^{-1}$), and (g) acetone (9 μl; 1/100 s and $f/8$; 46.6°C with $1.6°C\,mm^{-1}$). Three types of drop evaporation were identified based on the interfacial patterns observed by the laser shadowgraphy [5]: At room temperature, cyclohexane, ethyl

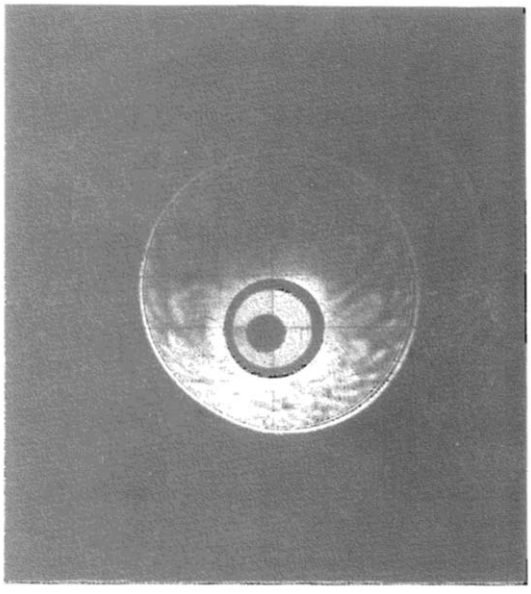

FIG. 8(a).

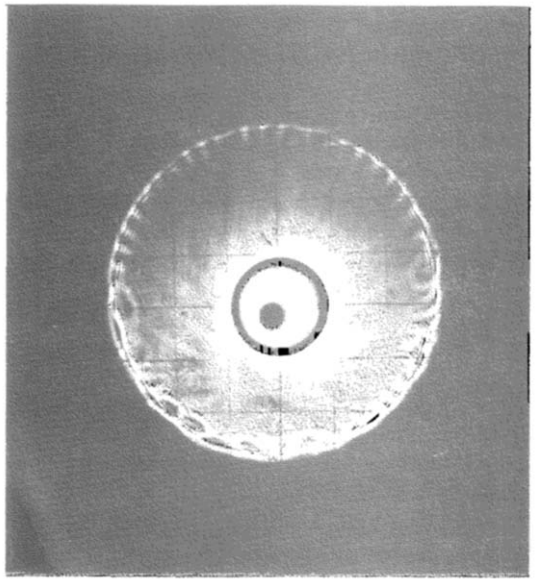

FIG. 8(b).

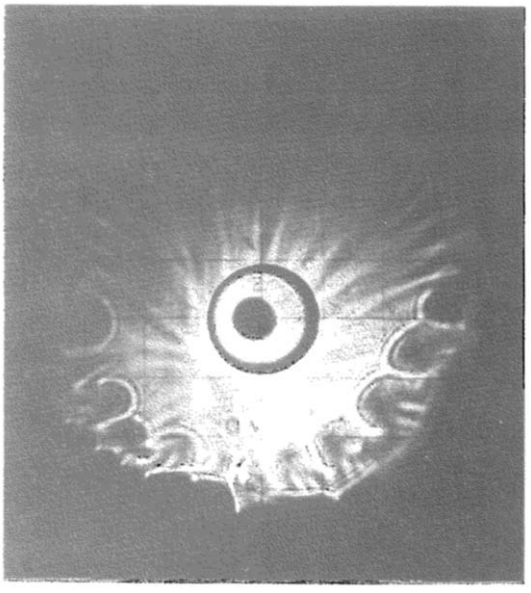

FIG. 8(c).

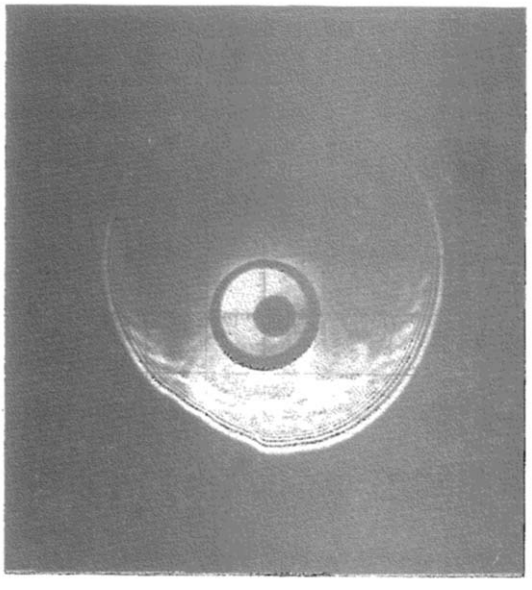

FIG. 8(d).

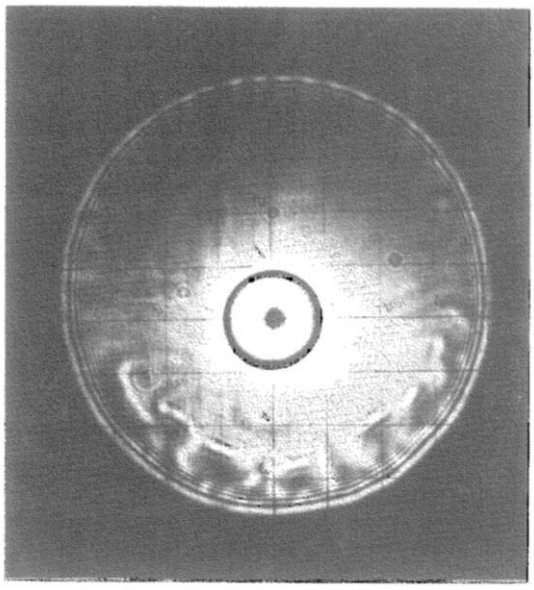

FIG. 8(e).

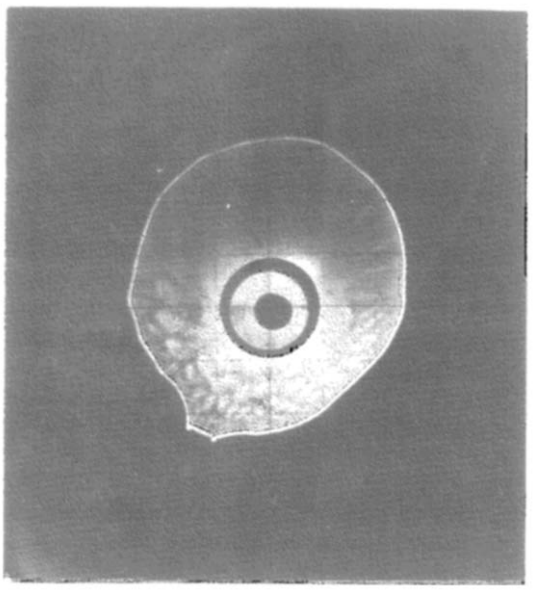

FIG. 8(f).

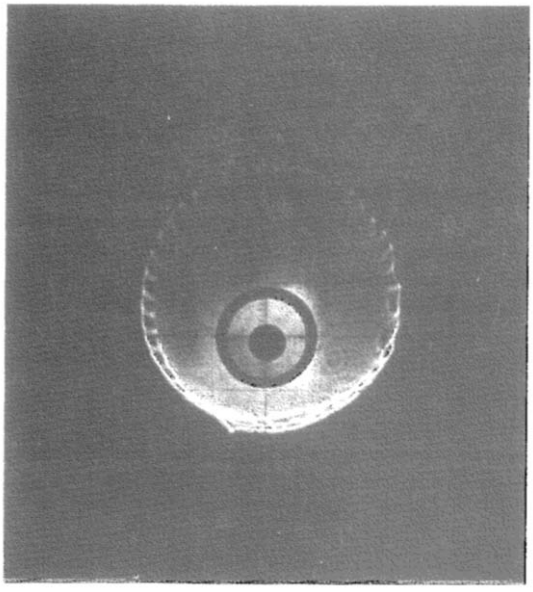

FIG. 8(g).

FIG. 8. Shadowgraphs of various liquid drops: (a) cyclohexane, (b) ethyl ether, (c) methylene chloride, (c) ethyl acetate, (e) chloroform, (f) benzene and (g) acetone.

ether, and carbon tetrachloride belong to the stable type; methylene chloride, ethyl acetate, chloroform and benzene are the substable type; and acetone is the unstable type. On the laser shadowgraph, the smooth surface of stable type drops forms a concentric circular image, while the rippled surface of an unstable type drop exhibits irregular radiant stripes within a sawtooth-like circle. The substable type drop has an image with the outer rings distorted from a circular shape and spiked. An interfacial flow regime map, a plot of the Marangoni number Ma versus the dielectric constant ε, was constructed to define the domain of the three basic interfacial structures. Since both Ma and ε tend to decrease with an increase in the liquid temperature T_l, the characteristics of drop vapor may change from the unstable to substable type or from the substable to stable type as the heating of drops is increased. An examination of the shadowgraphs in Fig. 8 reveals that both cyclohexane and ethyl ether remained the stable type while the chloroform drop at 51.3°C became the stable type. Similarly, methylene chloride, ethyl acetate and benzene remained the

substable type, while the acetone drop at 46.6°C became the substable type. All of the liquids had one thing in common: the warm side of the drop (upper part in the photos) was characterized by uniform temperature, indicating the occurrence of strong buoyancy driven convection, while the cold end was surface tension controlled as in the case of a carbon tetrachloride drop shown in Figs. 7(a)–(c). The effect of liquid properties is exemplified through different flow patterns in the lower part of the shadowgraphs: some photos exhibited a feather-like structure such as seen in the cyclohexane, ethyl acetate, benzene and chloroform drops when T_l was appreciably below the saturation temperature T_s. Other shadowgraphs had cellular structures near the image periphery such as was observed in the ethyl ether, methylene chloride and acetone drops when T_l was raised closer to T_s. All of the flow patterns varied with time. In general, cells began to appear at a certain value of T_l and the cell size grew with an increase in T_l toward T_s. It is still uncertain what internal flow forms are represented by a feather-like structure or cells in the shadowgraph.

2.2.4. *Effect of drop motion.* A nonuniform plate temperature such as depicted in Fig. 2 caused a surface tension temperature gradient $\partial\sigma/\partial T_l$ on the drop surface, where σ denotes the surface tension coefficient. When $\partial\sigma/\partial T_l$ reached a certain value, the drop would start a translatory motion (toward the colder side) on a horizontal plate. Figure 9 is a schematic diagram of flow patterns in a moving drop on a plate at slightly inclined (less than 4° angle) or horizontal position. Both $\partial\sigma/\partial T_l$ and plate inclination determine the speed of drop movement without altering the basic flow patterns.

Figures 4 and 9 are compared to determine the effect of drop motion: the induction of drop motion caused a weakening of the flow strength in both regions I and II which were respectively controlled by buoyancy and surface tension forces. The role of region III in mixing the warm with the cold streams was diminished, forming a nearly stagnant space at the drop summit. However, the path of flow stream for transporting the heat from the warm to cold sides in region II is stretched. Eventually, two vortices in region IV of a stationary drop were replaced by a new region IV consisting of a ring of small, 2-dim. roll cells for locomotion of the drop. In the moving drop, cold fluids of regions I and IV flowed down into the partition between the regions. The roll cells were clearly visible on the warm side where flow circulation was strong. The visibility of these roll cells was reduced toward the cold side due to the weakening of flow strength. There should exist concentric rings of roll cells near the liquid–solid interface in the interior of the drop but these were not detectable by the naked eye. These roll cells, with rotating strength diminishing from warm to cold sides, must be responsible for the drop to crawl on the test plate. Unfortunately, the theory could not be confirmed by the laser shadowgraphy due to difficulty in focusing the light on a moving drop. Due to the weakening of convective currents and mixing between the warm and cold streams, the evaporation rate is reduced in a moving drop.

2.2.5. *Effect of air–liquid interfacial geometry.* A minute drop on a plate takes a lens shape of curvature R. As a result of the curvature, a surface tension force of $2\sigma/R$ is induced on the air–liquid interface. This surface force does not exist in the case of an evaporating liquid layer, where the interfacial curvature is infinity. Berg *et al.* [1] observed that in a pool of evaporating liquid, the metamorphosis varies with depth from the regular (Bénard) cells to the larger cells in which a substructure of ribs appeared followed by the dismemberment of the cells into a network of sluggishly moving hot and cold streamers. Beyond a depth of 1 cm, no further changes in flow form could be discerned. The basic structural forms (cells, ribs, streamers) appeared in all liquids except water. The properties of the liquid affected the flow structures to a much lesser extent compared with the depth of the evaporating liquid. In contrast, there exists four patterns of flow structures in a minute drop evaporating on a plate of uniform temperature, as shown in Fig. 10 which is reproduced from ref. [6]: intensive convection current, cellular form, stagnation

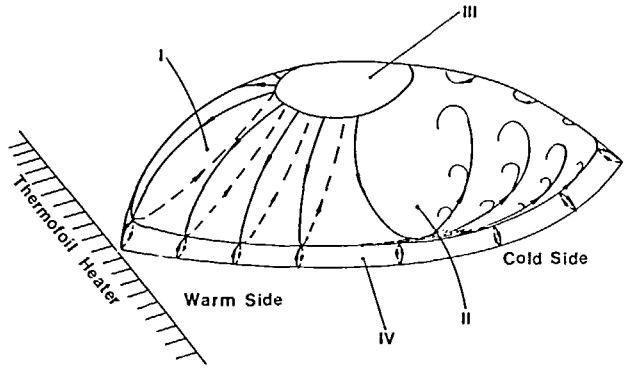

FIG. 9. A schematic diagram of flow patterns in a moving drop evaporating on a slightly inclined or horizontal plate with a temperature field.

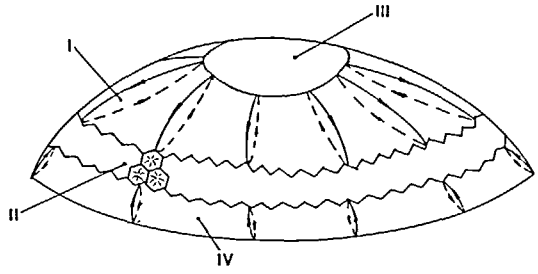

FIG. 10. A schematic diagram of a flow pattern in a stationary drop evaporating on a uniformly-heated horizontal plate.

and weak circulation in regions I–IV, respectively. In a liquid pool of the same depth as the diameter of these minute drops, about 2–3 mm, one would observe only cellular flow. The difference between a cellular structure in a liquid layer and the flow pattern in a drop, Fig. 10, may be attributed to the effect of the surface tension force $2\sigma/R$.

3. CONCLUSION

The solid suspension method has revealed a variety of flow regions in drops undergoing evaporative convection on an inclined plate with a temperature field. The convective pattern on the warm side is induced by a buoyancy driven instability, while that on the cold side is controlled by surface tension force. The major fraction of evaporation takes place on the warm side of the drop surface due to higher surface temperature and strong flow circulation. The flow regimes in between the warm and cold sides are governed by the combined effect of buoyancy and surface tension forces and are responsible for the exchange of heat between the warm and cold sides through mixing. Laser shadowgraphy has revealed the extent of interfacial turbulence and its results have confirmed the observations disclosed by the solid suspension method of flow visualization.

Drop motion alters some flow patterns in the four regimes and weakens both convective currents and stream mixing, resulting in a reduction in the evaporation rate. Liquid properties affect appreciably both the interfacial and internal flow structures and consequently alter the speed of drop evaporation. The contour of the air–liquid interface contributes to the complication of internal flow structures.

Acknowledgements—The work was supported by the National Science Foundation under Grant No. ENG-7816972.

REFERENCES

1. C. S. Sternling and L. E. Scriven, Interfacial turbulence; hydrodynamic instability and the Marangoni effect, *A.I.Ch.E. Jl* **5**, 514–523 (1959).
2. J. C. Berg, M. Boudart and A. Acrivos, Natural convection in pools of evaporating liquids, *J. Fluid Mech.* **24**, 721–735 (1966).
3. J. C. Han and Wen-Jei Yang, Thermal instability in liquid droplets on a heated surface, *J. Heat Transfer* **102**, 581–583 (1980).
4. J. C. Han and Wen-Jei Yang, Thermal instability in spherical liquid shells induced by surface tension, *Lett. Heat Mass Transfer* **7**, 363–378 (1980).
5. N. Zhang and Wen-Jei Yang, Natural convection in evaporating minute drops, *Trans. Am. Soc. Mech. Engrs*, Series C, *J. Heat Transfer* **104**, 656–662 (1982).
6. N. Zhang and Wen-Jei Yang, Evaporation and explosion of liquid drops on a heated plate, *Experiments in Fluids* (1983) in press.

CONVECTION EVAPORATOIRE POUR DES PETITES GOUTTES SUR UNE PLAQUE AVEC GRADIENT DE TEMPERATURE

Résumé—La convection thermique dans une petite goutte s'évaporant sur une surface plane est visualisée selon deux méthodes : suspension solide et méthode d'ombre par laser. La plaque est partiellement chauffée pour créer un champ de température sur la surface d'essai de façon que l'effet Marangoni puisse être induit sur la surface de la goutte. En modifiant l'inclinaison de la plaque, la goutte peut rester au même endroit ou se déplacer sur la plaque. L'observation des configurations d'écoulement dans une goutte stationnaire montre que la présence de la tension interfaciale et des forces d'Archimède conduit à quatre régimes distincts d'écoulement dans la goutte avec la convection pilotée par les forces d'Archimède sur le coté chaud et l'instabilité pilotée par la tension interfaciale sur le coté froid. Les effets du mouvement de la goutte, des propriétés du liquide et de la géométrie de l'interface air–liquide sur les structures d'écoulement interfacial et interne sont déterminés et on discute les conséquences de la vitesse d'évaporation.

VERDUNSTUNGSKONVEKTION IN SEHR KLEINEN TRÖPFCHEN AUF EINER PLATTE MIT EINEM TEMPERATURGRADIENTEN

Zusammenfassung—Die thermische Konvektion in einem sehr kleinen verdampfenden Tröpfchen auf einer ebenen Plattenoberfläche wird mit Hilfe von zwei Verfahren sichtbar gemacht: Suspensions- und Laserverfahren. Die Platte ist örtlich beheizt, um in der Versuchszone ein Temperaturfeld zu erzeugen, mit dem der Marangoni-Effekt auf der Tropfenoberfläche hervorgerufen werden kann. Durch unterschiedliche Plattenneigung kann erreicht werden, daß der verdampfende Tropfen in Ruhe an derselben Stelle bleibt oder sich auf der Platte bewegt. Die Beobachtung von Strömungsbildern in einem Tropfen offenbart, daß das Voehandensein der Oberflächenspannung einerseits und von Auftriebskräften andererseits zu vier unterschiedlichen Strömungszuständen im Tropfen führt, und zwar mit auftriebsbestimmter Konvektion auf der warmen Seite und durch Oberflächenspannung bedingte Instabilität auf der kalten Seite. Die Einflüsse von Tropfenbewegung, Flüssigkeitseigenschaften und der Phasengrenzflächengeometrie auf die Strömungsstrukturen an der Phasengrenze und im Inneren werden bestimmt und die Auswirkungen auf die Verdunstungsgeschwindigkeit erörtert.

ИСПАРИТЕЛЬНАЯ КОНВЕКЦИЯ В МЕЛЬЧАЙШИХ КАПЛЯХ НА ПЛАСТИНЕ ПРИ ВОЗДЕЙСТВИИ ТЕМПЕРАТУРНОГО ГРАДИЕНТА

Аннотация—Исследование тепловой конвекции в мелких каплях, испаряющихся на плоской поверхности, проведено лазерными теневыми методами путем визуализации суспензии твердых микрочастиц, введенных в каплю. Для создания температурного поля на исследуемом участке с тем, чтобы вызвать на поверхности капли эффект Марангони, пластину частично нагревали. При изменении наклона пластины испаряющаяся капля могла оставаться на месте или двигаться по пластине. Наблюдение за течением в неподвижной капле показывает, что в результате влияния поверхностного натяжения и подъемных сил в капле возникают четыре четко различимых режима течения с конвекцией под действием подъемной силы на нагретой стороне и неустойчивостью под действием поверхностного натяжения на холодной. Определено влияние движения капли, свойств жидкости и геометрии границы раздела воздух-жидкость как на структуру пограничного, так и внутреннего потока. Рассмотрено также влияние скорости испарения.